Journal of Zhejiang University-SCIENCE A (Applied Physics & Engineering)
ISSN 1673-565X (Print); ISSN 1862-1775 (Online)
www.zju.edu.cn/jzus; www.springerlink.com
E-mail: jzus@zju.edu.cn

Enhancement of ion transport in porous media by the use of a continuously reoriented electric field*

Juan ALMEIRA, Chang-sheng PENG†‡, Ahmed ABOU-SHADY

(*College of Environmental Science and Engineering, Ocean University of China, Qingdao 266100, China*)

†E-mail: cspeng@ouc.edu.cn

Received Jan. 10, 2012; Revision accepted Apr. 28, 2012; Crosschecked May 29, 2012

Abstract: Electromigration in porous media is enhanced by a new type of electrokinetic processing. Compared with a single-oriented electric field, a continuously reoriented electric field was proven to sharply enhance mass transport of several heavy metals in kaolin. The initial concentration of the metals was: Cd: 250 mg/kg; Cu: 250 mg/kg; Ni: 250 mg/kg; Zn: 900 mg/kg. Electric field reorientation was obtained by the use of a fixed anode and a cathode that rotated at different frequencies (0, 0.25, 1.00, 1.25, 2.00, 5.00 and 10.00 r/m). Mass transport evidently increased from 0 r/m to 1.25 r/m, and then decreased as the rotation speed reached 10 r/m. From 0 r/m to 1.25 r/m, mass transport increased 2.87 times for Cd, 3.17 times for Cu, 2.11 times for Ni, and 4.13 times for Zn. We suggest that continuous reorientation of the electric field facilitates the advance of ions through kaolin pores, minimizing the retardation effect caused by media tortuosity.

Key words: Electromigration, Heavy metals, Kaolin, Electric field orientation, Tortuosity, Rotating electrodes
doi:10.1631/jzus.A1200017 **Document code:** A **CLC number:** TQ15

1 Introduction

The transport of charged particles in porous media in an electric field has numerous applications including soil chemistry (Yuan and Weng, 2006), ion exchange (Lemaire *et al.*, 2010), biotechnology (Goering, 2010), membrane science (Sadrzadeh *et al.*, 2007), electrophoresis (Puig *et al*., 2007), and chromatography (Humble *et al*., 2007). For some of these applications, the net speed at which the charged particles approach the electrodes becomes a limiting factor. For example, the removal of heavy metals from soil by in-situ soil electrokinetic remediation (EKR), which is achieved mainly by electromigration and to a lesser degree by electroosmosis (Probstein and Hicks, 1993), might take several years (Lageman *et al*., 2005). The term 'net speed' is used here because in porous media the trajectory of the charged particles towards the electrodes is not straight; for this reason, the speed at which a particle actually approaches an electrode depends on the strength of the electric field, but is also reduced by the media tortuosity. This is probably one of the main difficulties when applying soil EKR outside the laboratory. In soil remediation practice, the use of a simple electric field for contaminant removal is seldom a complete solution. Frequently, the electric field is coupled with the action of bacteria, as in the Lasagna process, or the addition of chemical substances such as surfactants, chelators or strong acids. In other applications, in order to promote microbial activity and reduce viscosity, even a quite expensive method in terms of energy consumption has been derived from the use of electrodes for soil treatment: ohmic heating of the soil by the introduction of over-potential.

Tsang (1984) and Shen and Chen (2007) have described how tortuosity appreciably slows down

‡ Corresponding author

* Project supported by the Ministry of Education of China (No. 708060), the Cultivation Fund of the Key Scientific and Technical Innovation Project, and the Program for New Century Excellent Talents in University, Ministry of Education (No. NCET-08-0508), China

water and solute flux in porous media. In a similar way, the tortuosity of a given medium could delay the transport of species driven by an electric field (i.e., electromigration). According to Jacobs *et al*. (1994), both electromigration velocity and electroosmotic velocity are affected by tortuosity. Eq. (1) describes electromigration velocity $U_{e,i}$ as a function of the mobility v_i, the charge number z_i, the local electric field ϕ, the tortuosity τ, and the Faraday constant F. Eq. (2) (the Helmholtz-Smoluchowski relation) describes electroosmotic velocity as affected by the permittivity of the solution ε, the zeta potential ζ, the tortuosity τ, the viscosity μ, and the local electric field ϕ. In these equations, tortuosity is interpreted as the ratio between the actual distance that a particle travels through a chaotic distribution of pores, and the straight-through distance along the pore matrix, ignoring the particle's constant change of course.

$$U_{e,i} = -\frac{v_i z_i F}{\tau}\left(\frac{\delta\phi}{\delta z}\right), \tag{1}$$

$$U_{eo} = \frac{\varepsilon\zeta}{\tau\mu}\left(\frac{\delta\phi}{\delta z}\right). \tag{2}$$

In this definition of electromigration speed, it is not explicit whether a particle can stop under the action of the electric field. In our description of electromigration, a particle can change its trajectory but, most importantly, it can also be stopped for some time during its journey towards the electrode. An additional function can be included to calculate the effect of particle blocking. This, however, may be the direction of further work.

We have hypothesized that, since there are narrow and irregular spaces between the particles forming any porous matrix, for a particle to move through, it should constantly change its direction. However, if the force vectors acting over the ions have a single direction, migration can occur only until the ions collide with an obstacle along their trajectory. In that case, the charged particles can continue traveling only if the force direction is conveniently changed every time the particle finds an obstacle. For this reason, it is proposed that constant reorientation of the electric field could increase ion flux caused by electromigration.

In electrokinetic common practice and other applications, a single-direction electric field is applied to transport charged particles towards electrodes. In this experiment, the use of a continuously reoriented electric field was evaluated for the removal of cadmium, copper, nickel and zinc from kaolin. The reorientation of the electric field was achieved via rotating electrodes.

2 Electric field reorientation

Rotating electrode reactors have been used since 1906 (Perkin, 1906; Price and Judge, 1906). Electrode rotation can accelerate electrochemical reactions mainly by increasing mass transfer at the electrodes. In static electrodes, the electrolyte flow at the electrode surface is caused solely by diffusion and convection, but with the use of rotating electrodes, the electrolyte flow regime can be modulated. Unlike regular rotating electrode reactors, in this study enhancement of mass transfer at the electrodes caused by electrode rotation was negligible because the speed of electrode rotations was quite slow. The sole aim of electrode rotation was to affect the orientation of the electric field.

The use of rotating electrodes is advantageous because it enables alterations to be made to the electric field using only a pair of electrodes, limiting the area where ions are to be finally collected. For instance, rotating the cathode brings about multiple electric field patterns. Fig. 1 presents the resultant electric field lines at two arbitrary times during cathode rotation. This representation was made with the assistance of Integrated Engineering Software (Canada), Coulomb 3D. At the first position (Fig. 1a), the electrodes' longitudinal axes are parallel, while at the second, the electrodes' longitudinal axes form a 90° angle (Fig. 1b). From this representation of the electric field, the following characteristics can be deduced: (1) greater deflections of the electric field lines occur close to the rotating electrode, i.e. the cathode; (2) the electric field orientation near the anode remains nearly unchanged; (3) in the central area of the electrokinetic cell the deflection of the electric field lines is minor. Therefore, enlarging the distance between the electrodes may result in a bigger cell area in which the electric field is altered by only a small degree.

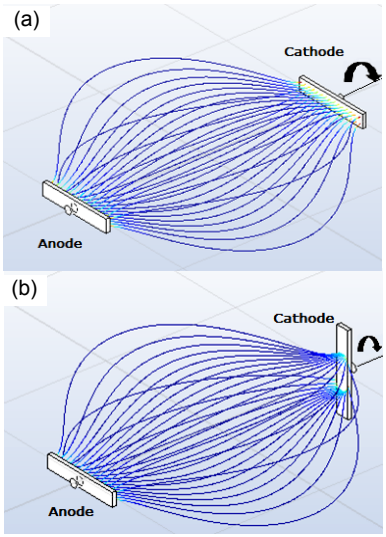

Fig. 1 Electric field lines pattern when the longitudinal axes of the electrodes are parallel (a) or forming a 90° angle (b)

Fig. 2 presents a conceptualization of ion electromigration when applying a single oriented electric field (Fig. 2a) and a continually reoriented electric field at two different arbitrary frequencies (Figs. 2b and 2c).

The arrows show three selected pathways between the kaolin sheets for which reorientation of the electric field could effectively facilitate ion advance towards the electrodes. For the uniform electric field, ions cannot easily change their direction, which evidently delays their migration. However, when the electric field orientation changes at a certain frequency, the direction of the ions can be easily adjusted and migration is substantially improved. As represented in Figs. 2b and 2c, the frequency at which the electric field orientation is changed plays an important role, because beyond a certain threshold the amplitude of the electric field orientation oscillations tends to zero; this clearly reduces the probability of the particles finding a path towards the electrodes.

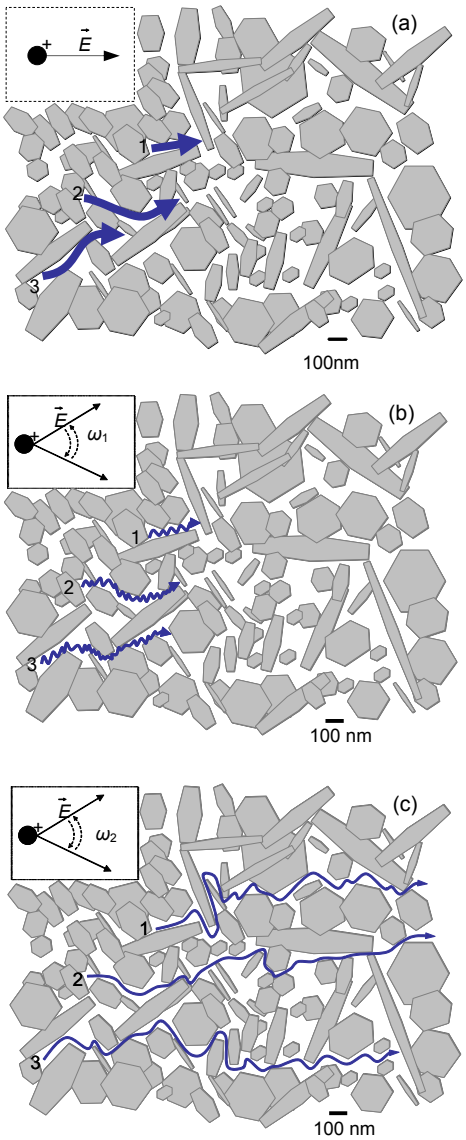

Fig. 2 Concept of ion electromigration through kaolin sheets for a single oriented (a) or constantly reoriented electric field at frequencies ω_1 (b) and ω_2 (c)
Kaolin sheets were digitized based on SEM photography of the kaolin used in this experiment. The numbers 1, 2 and 3 represent the expected particle trajectories

3 Materials and methods

3.1 Design of the electrokinetic cell

The main body of the cell consisted of a Plexiglas tube in which kaolin was packed (Fig. 3). The inner diameter of the cell tube was 19 mm. Two working electrodes were installed, one at each end of the tube. To avoid corrosion, titanium electrodes with iridium and ruthenium oxide coatings were used. The electrodes were 18.0 mm long, 4.0 mm wide, and 1.2 mm thick. They were supported at their mid-point by a titanium screw. The cathode-holding titanium screw was connected to an electric motor (provided by the Longer Pump Ltd., China) through which the rotating speed of the cathode was controlled. The frequency at which the electric field orientation changed was adjusted by controlling the rotating speed of the cathode.

To avoid water leakage, the electrodes were attached to a rubber plunger, which subsequently was fitted into the cell tube. The distance between the working electrodes was 66 mm (Fig. 3b). Two reference electrodes, made of titanium and located at the mid-point between the working electrodes, were employed to measure voltage drop through the cell.

The kaolin sample was held in position by two filter membranes, one on the anode side and the other on the cathode side. On the anode side, a nylon mesh (pore size=0.05 mm) was employed both to fix the sample and to facilitate acid front advance. Similarly, on the cathode side, a three layer filter-membrane was used to slightly retard base front advance (Virkutyte and Sillanpaa, 2007). This membrane was composed of a mixed cellulose ester (MCE) inner layer (pore size=0.1 μm) covered by two polypropylene (PP) layers (pore size=8 μm), one on each side. The two membranes were attached to the cell inner wall by a polyvinyl chloride (PVC) ring that stretched the membrane in a drum-like structure (Fig. 3). A space was left between the membranes and electrodes in which to build the electrode chambers.

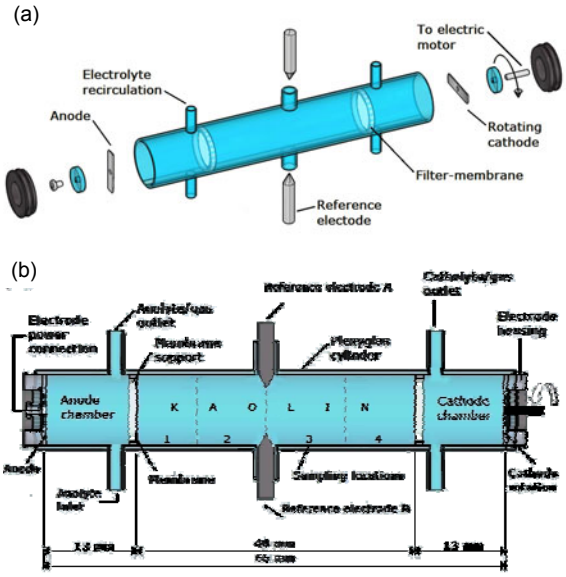

Fig. 3 3D model (a) and longitudinal cross section view (b) of the electrokinetic cell

3.2 Experimental set-up

Each electrode chamber was provided with an electrolyte reservoir and an overflow reservoir, both made of PVC (Fig. 4). The reservoirs had a maximum capacity of 20 ml. To allow electrolyte recirculation between the reservoirs and the electrode chambers, each electrode chamber was connected to its respective electrolyte reservoir by two polyurethane tubes (inner diameter=2.50 mm). The first tube connected the bottom of the electrode chamber to that of the electrolyte reservoir to form an electrolyte inlet. The second tube connected the top of the electrode chamber to the bottom of the electrolyte reservoir as an electrolyte/gas outlet. In addition, to ensure electrolyte circulation between the electrode chambers and the electrolyte reservoirs as well as the permanent evacuation of the gas produced, a peristaltic pump (BQ-50, Longer Pump Ltd., China) with a flow rate of 207 ml/h was installed at each of the gas/electrolyte outlet tubes. Finally, each overflow reservoir was connected to its electrolyte reservoir by a polyurethane tube (inner diameter=2.50 mm) that connected the top of the electrolyte reservoir to the top of the overflow reservoir (Fig. 4).

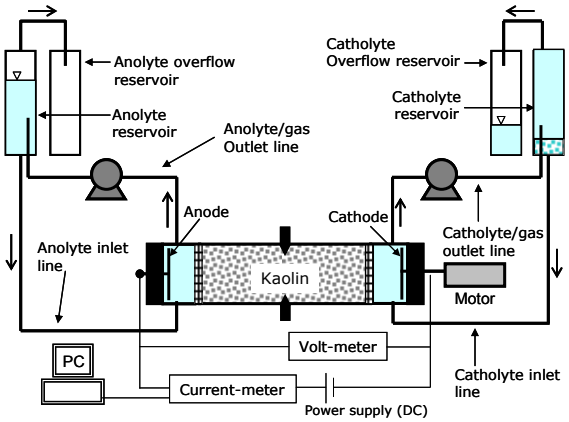

Fig. 4 Electrokinetic testing set-up

The electrolyte reservoirs were covered to avoid excessive water evaporation but allowing the release of gas (i.e., oxygen and hydrogen) produced at the electrodes. The electrode reservoirs were kept at the same height to avoid any difference in hydraulic static pressure over the sample.

A DC power supply (PS-303D, Hong Kong Longwei Instruments Ltd. Co., China) was used for this experiment. Its voltage range was 0.5–30.0 V and current range 0.1–1.0 A.

3.3 Sample preparation

Commercial kaolin purchased from the Shanghai Ludu Chemical Reagent Factory Co., China was used

for this experiment. This kaolin is extracted from Suzhou deposits in Jiangsu Province, China. Kaolin was used because of its homogeneity, relatively low cationic exchange capacity, fine grain distribution, and low permeability. Furthermore, kaolin has been widely used in the study of the electrokinetic treatment of soil as it provides a reproducible, low buffering clayey model soil (Pamukcu *et al*., 2004; Wang *et al*., 2007; Yeung *et al*., 2011). The elevated concentration of sulfates (Table 1) in kaolin and the associated low pH are most probably attributable to the addition of sulfuric acid during the bleaching process in typical kaolin industrial processing (Wilson, 2004). The purchased kaolin had an anomalous high concentration of zinc of 900 mg/kg.

Table 1 Characterization of Suzhou kaolin

Item	Description
Name	Suzhou kaolin
Soil classification (ASTM D-2487)	Clay
Hydraulic conductivity (ASTM D-7100) (cm/s)	1.1×10^{-8}
Particle size distribution	
Clay	100%
Atterberg limits (ASTM D-4318)	
Plastic limit	32%
Liquid limit	78%
pH (9045D US EPA, in water)	3.76
Conductivity (in water) (μS/cm)	1485
Cation exchange capacity (9081 US EPA) (μg/g)	1326
Zinc (mg/L)	900
Arsenic (from fabricant) (mg/kg)	2
Lead (from fabricant) (mg/kg)	10
Chlorides (from fabricant) (mg/kg)	370
Sulfates (mg/kg)	1705
Organic mater (ignition at 400 °C)	2%
Bulk density (mg/ml)	1.43

The kaolin was first dried at 105 °C for 24 h and then mixed at a 1:1 water/soil ratio with a solution containing cadmium sulfate, copper sulfate and nickel sulfate (all purchased from the Sinopharm Co. Ltd., China) prepared with deionized water. This solution contained 250 mg/L of cadmium, 250 mg/L of copper and 250 mg/L of nickel. After this operation, the kaolin sample became liquid, and was manually mixed using a polyethylene spatula until homogeneity was reached. It was then air dried for 4–5 d until it reached a gravimetric water content (i.e., solid/liquid ratio) of 66%.

3.4 Electrokinetic experiments

First, the kaolin was packed into the electrokinetic cell, and the membranes were installed with a mechanical device. Then, the electrodes and electrolyte reservoirs were mounted. The anolyte and catholyte reservoirs were first filled with 0.01 mol/L KNO_3. Later, the electrodes were connected to the power supply and direct current was applied at a constant voltage of (2.0±0.1) V/cm (i.e., 13.2 V) for 48 h. For each experiment, the cathode was rotated at different speeds, namely 0 r/m, 0.25 r/m, 1.00 r/m, 1.25 r/m, 2.00 r/m, 5.00 r/m and 10.00 r/m, whereas the anode remained static.

3.5 Analytical methods

The electric current was measured with a digital ammeter (UT-60E, UNI-T) linked to a personal computer (PC). With the computer system, it was possible to read and record current values every hour. In addition, the voltage between working electrodes and that between working and reference electrodes (i.e., the voltage drop) were manually measured with a digital voltmeter (UT-60E, UNI-T). The voltage drop was measured between the anode and reference electrodes for the half of the cell next to the anode (i.e., on the anode side). Likewise, it was measured between the cathode and reference electrodes for the half of the cell next to the cathode (i.e., on the cathode side).

After electrokinetic testing, the sample was extruded from the electrokinetic cell using the same mechanical device used for its packing. Then it was cut into (10±1) mm thick slices. The pH, conductivity, and Cd, Cu, Ni and Zn concentrations were measured in each slice. Conductivity and pH were measured daily in the electrode chambers. The remaining amounts of metals were also determined in the working electrodes, membranes, anolyte and catholyte.

Kaolin conductivity and pH were both measured at a 1:2 soil/water ratio. The pH was measured according to the 9045D (US EPA) method. The pH and conductivity of the electrolytes were measured directly from their respective solutions.

According to the 7130 US EPA (atomic absorption, direct aspiration) method, cadmium concentration was determined by flame atomic absorption (FLAA) using a Thermo Scientific iCE 3300 AA spectrometer. Kaolin samples were previously

digested as described in the method 3050B (US EPA). The applied acid digestion is not a complete digestion, but one in which only environmentally available elements are recovered.

To ensure the quality of the data, the following precautions were taken throughout the experiment: (1) analytic grade reagents were used; (2) all chemical analyses were performed in duplicate; (3) the current was continually recorded each hour; (4) voltage drop was measured twice for each reported value; (5) new electrodes, tubes, reservoirs, and membranes were used for each test, and the electrokinetic cell was soaked overnight in a nitric acid solution (pH=2.0) before each new test. In addition, to reduce the amount of natural resources consumed in this experiment, the treated samples were kept as small as possible.

4 Results and discussion

4.1 Heavy metals electromigration

It was assumed that ion migration observed during the experiment was achieved mainly by electromigration. The registered electroosmotic flow did not surpass (0.4±0.25) ml, equivalent to 5.0% of the pore fluid volume ((8.0±0.25) ml), in any of the performed tests. This was most probably the result of a low zeta potential (ζ), caused by the high initial concentration of ionic species.

Given that pH was not controlled, accumulation of hydroxides near the cathode was present in all the runs. But, even with the accumulation of hydroxides near the cathode and the resultant lowering in conductivity, important differences in ion electromigration were observed throughout the experiment. The amount of ions that migrated and was deposited near the cathode was closely related to the cathode rotation speed. Mass transport towards the cathode increased considerably at cathode rotation speeds between 0.25 r/m and 1.25 r/m (Fig. 5). However, electromigration decreased again between 1.25 r/m and 10.00 r/m, showing a small peak at 5.00 r/m. It appears that when the field orientation was changed too fast, the direction of the force acting over the ions was constantly changing just before cations could make any significant displacement in the direction of the cathode.

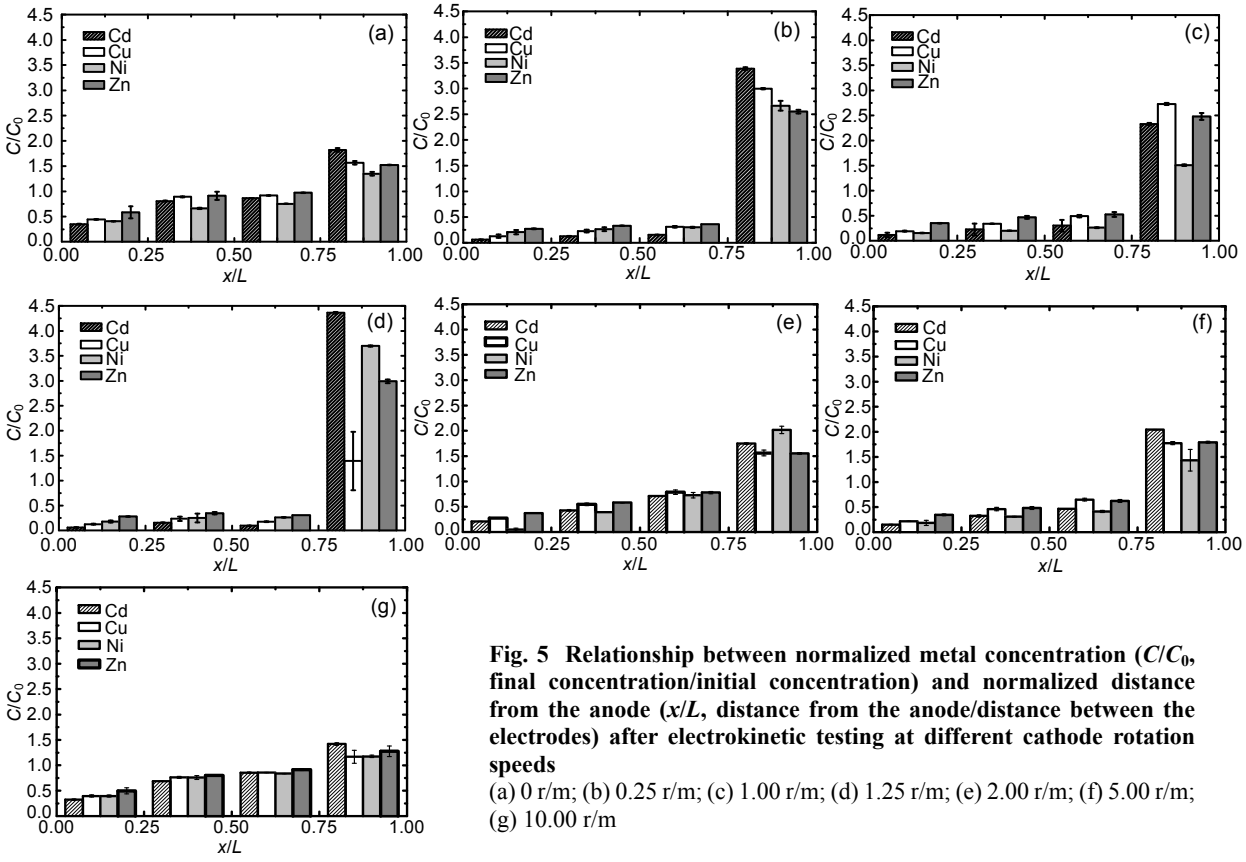

Fig. 5 Relationship between normalized metal concentration (C/C_0, final concentration/initial concentration) and normalized distance from the anode (x/L, distance from the anode/distance between the electrodes) after electrokinetic testing at different cathode rotation speeds

(a) 0 r/m; (b) 0.25 r/m; (c) 1.00 r/m; (d) 1.25 r/m; (e) 2.00 r/m; (f) 5.00 r/m; (g) 10.00 r/m

Thus, lowering the cathode rotation speed increased the net displacement of ions in the direction of the cathode.

Ion electromigration closely followed the electrical current curves (Fig. 5 and Table 2). At the highest current values, massive electromigration was detected. Hence, the highest values for electromigration were found from 0.25 r/m to 1.25 r/m, with 1.25 r/m giving the highest value overall. At 1.25 r/m, mass transport increased 2.11 times for nickel, 2.87 times for cadmium, 3.17 times for copper and 4.13 times for zinc compared with the static cathode (i.e., 0 r/m), respectively (Table 2).

Table 2 Total mass transport at different cathode rotation speeds

Cathode rotation speed (r/m)	Total migrated (mg)			
	Cd	Cu	Ni	Zn
0	0.8	0.6	0.9	1.5
0.25	2.0	1.8	1.7	5.5
1.00	1.7	1.4	1.7	4.2
1.25	2.3	1.9	1.9	6.2
2.00	1.1	1.0	1.3	3.1
5.00	1.7	1.4	1.7	4.5
10.00	0.9	0.8	0.8	2.2
Mass transport increment ratio between 1.25 and 0 r/m	2.87	3.17	2.11	4.13

Naturally, mass transport of Zn was greater because it had higher availability (i.e., concentration). The electromigration values observed at 0 r/m and 10.00 r/m show the influence of the frequency at which the electric field was changed. The weight of electromigrated metals at these two speeds was nearly the same, which shows that the effect of cathode rotation reaching 10.00 r/m was negligible (Table 2).

For most cathode speed rotations, more cadmium migrated towards the cathode than any other metal (Fig. 5). In contrast, for copper, nickel and zinc, a consistent sequence indicating their ease of migration was not evident. However, at 0.25 r/m and 1.25 r/m such a sequence was well-defined: Cd>Cu> Ni>Zn. This sequence differs from that found by Nystroem *et al*. (2005) and Cox *et al*. (1996), except for the position of cadmium.

The flow regime at the electrode surface, which was determined by the Reynolds number, depends on several factors including viscosity, electrode geometry, and rotation speed (Eisenberg *et al*., 1954; Fabian *et al*., 2006). The Reynolds number was calculated by $Re=\rho ND^2/\mu$, as described by Sinnott (1983), where ρ denotes the fluid density (kg/m^3), N is the electrode speed in revolutions per second (r/s), D is the diameter of the electrode (m), and μ is the fluid viscosity (N·s/m^2). Small Reynolds numbers were obtained: the lowest was 2, at 0.25 r/m, and the highest was 61, at 10 r/m. Thus, the flow regime was always laminar. Furthermore, for a rotating electrode reactor such as the rotating cylinder electrode (RCE), the Reynolds number and mass transport enhancement (γ) can be related by $\gamma=Re^{0.18}$ (Gabe *et al.*, 1998). Above all, our results suggest that for the electrokinetic cell, mass transfer was not exponentially related to the flow regime at the electrodes. For this reason we believe that the regime flux at the electrodes did not have a major influence on mass transfer.

As reported by Moldrup *et al*. (2001), liquid phase tortuosity can be affected by the volumetric water content θ=moisture content×soil bulk density. For the performed runs, θ dropped moderately from 94% to 82% on average, which corresponds to a tortuosity value of around 2. Tortuosity may have even higher values in field applications where the stability of the terrain demands much lower water contents. In such cases, the possibility of modifying the electric field orientation may represent an even greater advantage.

4.2 Current density

Notably stable curves of current density were obtained when the cathode was rotating (Fig. 6a). In contrast, current density was very unsteady when the cathode and the anode were static. The increase in current at certain speed rotations clearly indicates a reduction in the sample resistance. This appears to be associated with the continuity of ion migration occurring when the electric field orientation was continually changed. Since ions transport the charges, reducing the probability of ions becoming stacked gives a more steady flow of charge towards the electrodes.

Current density was the highest in the 0.25–1.25 r/m range. Above 1.25 r/m, it decreased, showing a smaller peak at 5.00 r/m. At 10.00 r/m the current was even lower than when the electrodes were static. These observations suggest that for different electrode rotation speeds there is a given *probability*

(Tsang, 1984) that the ions will have a smoother journey towards the electrodes. Such a probability had its highest value between 0.25 r/m and 1.25 r/m.

Notable differences were found when comparing the total charge flow through the cell (in coulombs, C) from 0 r/m to 10.00 r/m (Fig. 6b). The most noticeable effect of cathode rotation was found between 0 r/m and 0.25–1.00 r/m: the total transported charge jumped from 202 C at 0 r/m to 475 C at 0.25 r/m, and to 476 C at 1.00 r/m. The charge transport was 2.4 times bigger than that from the static electrodes. When the cathode speed rose further to 2.00 r/m, the charge began a downward trend.

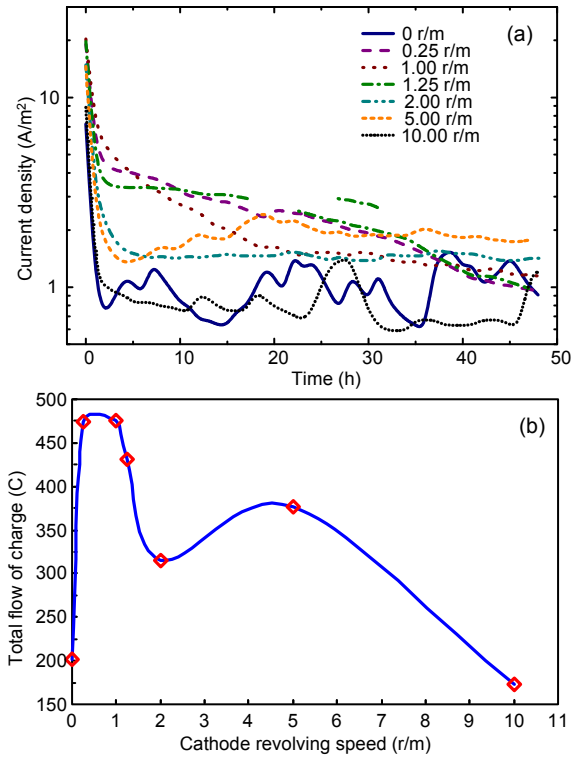

Fig. 6 Current density vs. time (a) and total charge flow through the cell (b) at different cathode rotation speeds

Hydrogen and oxygen gas produced at the electrodes may insulate the electrodes. Once hydrogen and oxygen are produced, they tend to remain on electrode surfaces as small bubbles, increasing electrode potential and lowering the current. The shear stress over such bubbles on the electrode surfaces will be intensified with the electrode rotation speed, causing them to fade out, thereby increasing electron transfer (Lorimer *et al*., 1997). In this case, in our experiment, charge transport (i.e., current) must have increased with the electrode speed. However, the current did not gradually increase with the cathode speed, but changed irregularly. Current values at 10.00 r/m were even lower than those at 0 r/m. Also, no change was noticed in the appearance of bubbles on the cathode's surface. Cathode and anode remained covered by bubbles in all tests. For these reasons, we suggest that electron transfer was influenced by interactions occurring in the porous matrix rather than in the electrode-electrolyte interface.

The discrepancy in the measured electrical current and electromigration between static and rotating electrodes at different speeds makes our hypothesis plausible. However, more direct measures and physical modeling will be needed before other possibilities can be ruled out. The mechanism under which this method achieves greater electromigration is not understood completely. A quantitative analysis will be published elsewhere.

4.3 Acid and base front advance

The pH at the anode chamber followed a similar trend for all cathode rotation speeds (Fig. 7). From 0 r/m to 10.00 r/m, pH decreased rapidly during the first 15 h to 2.5±0.5, then remained nearly constant for the rest of the test. Even though pH values were similar at the anode chamber, the pH of kaolin changed with the cathode rotation speed. Such changes in pH may indicate a wider spreading of the acid front for certain cathode rotation speeds. From 0.25 r/m to 1.00 r/m the acid front was widely spread while for 2.00 r/m and 5.00 r/m the spread was minor. For 0 r/m and 10.00 r/m, the pH of kaolin remained fairly close to its initial value. Thus, the migration of H^+ was affected by the fluctuation of the electric field orientation, as happened for Cd, Cu, Ni and Zn.

If the reorientation of the electric field effectively reduces the probability of the ions becoming stacked in dead end pores, then how can ions travel throughout the pores when the electric field has a single direction. Electroosmosis can substantially aid the transport of dissolved ions. Also, when electroosmosis is not significant, the acid front (i.e., H^+ ions migrating towards the cathode) works like a mobile phase in chromatography, eluting ions from the porous matrix (Shen *et al*., 2007). Furthermore, the transient behavior of the electric field, which can change locally depending on ion concentration and

pH, may also help ions move through a pore network (Probstein and Hicks, 1993).

Regarding the base front, we obtained lower production of OH^- ions at 0 r/m and 10.00 r/m. This might have been caused by lower conductivity at these rotation speeds. The production of OH^- ions was much slower at 0 r/m, followed by 10.00 r/m. The pH curves of the catholyte from 0.25 to 5.00 r/m were hardly distinguishable.

The pH of the kaolin close to the cathode did not exceed 7.0. Therefore, precipitation of most metals most likely occurred in the kaolin layer just next to the cathode side membrane. As the mass balance confirmed (Table 3), on average 90% of the metals remained in the kaolin sample and 10% was deposited on the cathode side membrane. We expect that controlling the pH could make more evident the effect of constantly reoriented electric field.

4.4 Changes in conductivity

The changes in conductivity observed in the electrolytes were related mainly to the existing pH conditions (Fig. 8a). At the anode chamber, high conductivity followed the high pH values observed from 0.25 r/m to 1.25 r/m; the values read at 2.00 r/m and 5.00 r/m corresponded to an intermediate level of

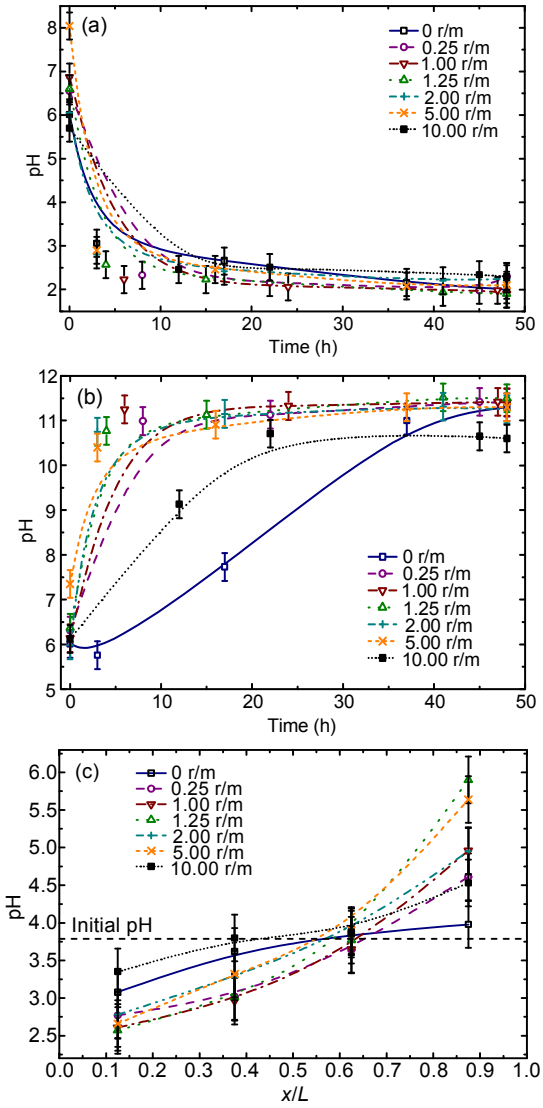

Fig. 7 pH at the anode (a), cathode (b) chamber and kaolin treated sample (c) at different cathode rotation speeds

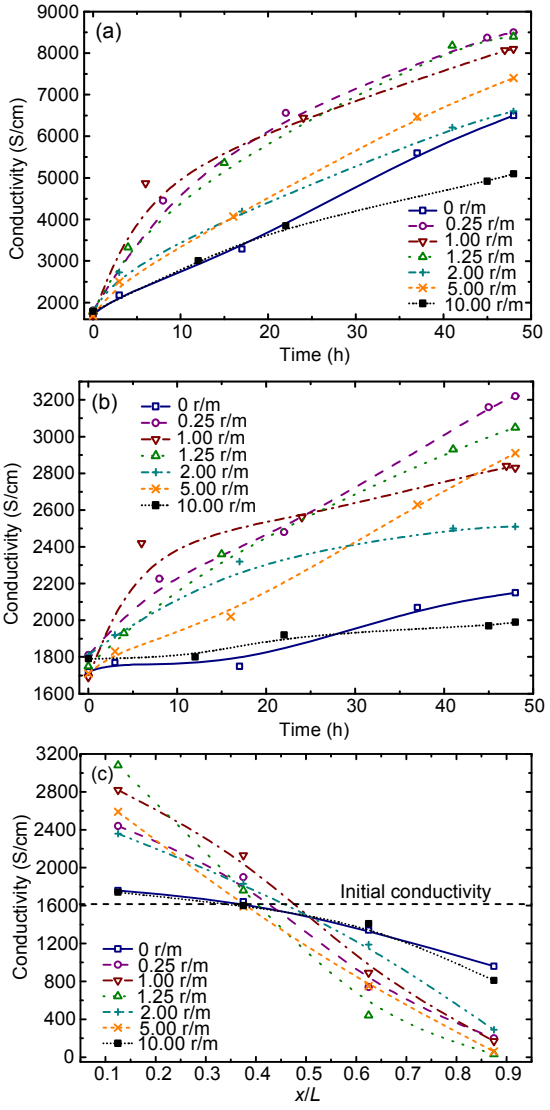

Fig. 8 Electrical conductivity at the anode (a), cathode chamber (b), and kaolin (c) at different cathode rotation speeds

Table 3 Material balance indicating how much Cd, Cu, Ni and Zn remained in each part of the electrokinetic cell at different cathode rotation speeds

Metal	Rotation speed (r/m)	Initial present (mg)	Remaining in kaolin (mg)	Anolyte (mg)	Catholyte supernatant (mg)	Catholyte precipitated (mg)	Cathode side membrane (mg)	Cathode (mg)	Total detected (%)
Cd	0	3.29	3.35	0.06	0	0.15	0.11	0.01	112
	0.25	3.14	3.30	0	0	0.13	0.16	0	114
	1.00	3.13	2.73	0.02	0	0.10	0.10	0.01	94
	1.25	3.09	2.80	0.01	0	0.09	0.18	0.01	100
	2.00	3.06	2.63	0.05	0	0.06	0.24	0.01	98
	5.00	3.23	2.36	0.03	0	0.09	0.26	0	85
	10.00	3.19	2.69	0.1	0	0.08	0.17	0.01	95
Cu	0	3.29	3.27	0.17	0	0.09	0.12	0	111
	0.25	3.14	3.19	0	0	0.08	0.13	0.01	109
	1.00	3.13	3.40	0.11	0	0.07	0.06	0.01	117
	1.25	3.09	3.04	0.08	0	0.06	0.16	0.01	108
	2.00	3.06	2.64	0.08	0	0.04	0.19	0	97
	5.00	3.23	2.48	0.03	0	0.06	0.22	0.01	86
	10.00	3.19	2.57	0.11	0	0.07	0.18	0.01	92
Ni	0	3.29	2.74	0.05	0	0.15	0.11	0.01	93
	0.25	3.14	2.97	0	0	0.13	0.15	0	104
	1.00	3.13	1.91	0.02	0.01	0.11	0.07	0	68
	1.25	3.09	2.73	0.01	0	0.10	0.18	0	98
	2.00	3.06	2.77	0.02	0.02	0.05	0.22	0.02	99
	5.00	3.23	1.86	0.02	0	0.09	0.27	0	69
	10.00	3.19	2.56	0.09	0	0.10	0.18	0	92
Zn	0	11.84	12.22	0.33	0.01	0.38	0.35	0.01	112
	0.25	11.31	10.84	0	0.02	0.31	0.47	0.01	103
	1.00	11.26	12.15	0.18	0.02	0.29	0.10	0.01	113
	1.25	11.14	9.07	0.16	0.03	0.25	0.58	0.02	91
	2.00	11.00	9.76	0.33	0	0.16	0.66	0.01	99
	5.00	11.64	9.30	0.17	0.01	0.25	0.74	0	90
	10.00	11.48	10.18	0.38	0	0.28	0.51	0.02	99

conductivity; finally, conductivities at 0 r/m and 10.00 r/m were located at the lower end of the scale, limiting the splitting of water at the electrodes. At the cathode chamber (Figs. 7b and 8b), for all runs, pH went beyond neutral pH in less than 15 h, while conductivity continued increasing during the remaining time. Provided that migration of positive ions through the membrane was limited, we deduce that precipitation of hydroxides at the cathode chamber was insignificant. For this reason, the production of OH^- resulted in an increase of conductivity in the cathode chamber. The conductivity curves for the catholyte showed trends similar to those of the anolyte: The lowest conductivity was obtained at 0 r/m and 10.00 r/m, the middle level at 2.00 r/m and 5.00 r/m, and the upper level from 0.25 r/m to 1.25 r/m.

The changes in conductivity across the sample were closely related to the changes in pH. Two main tendencies were observed: at 0 r/m and 10.00 r/m, conductivity remained very close to the initial value; from 0.25 r/m to 5.00 r/m, conductivity tended to zero near the cathode (Fig. 7 and Fig. 8)

Distinctly low electrical conductivities near the cathode may be a sign of metal hydroxide precipitation. Depolarization of the cathode will be carried out in further experiments. In this study, the idea was to keep the system as simple as possible, avoiding violent changes in conductivity caused by the addition of cathode depolarizing agents such as acids. For instance, the addition of nitric acid for cathode depolarization causes such big changes in conductivity that the variations in electrical current or ion migration caused by the rotation of the cathode would be more difficult to detect.

4.5 Voltage drop along the sample

From Ohm's law, a higher resistance will cause a greater voltage drop. Even when we did not measure voltage changes at the pore scale, from the voltage drop along the anode and the cathode sides it was possible to infer resistance changes of a minor scale along the electrokinetic cell.

Metallic hydroxides deposited mainly next to the cathode side membrane brought about a permanent high voltage drop along the cathode side in all runs. The difference between a static and a rotating cathode was measurable, especially during the first 10 h, before the pH surpassed 7.0 in the catholyte. When the cathode was not rotated, the voltage drop was the greatest overall, even when the catholyte pH was the lowest (Fig. 9b). The lowest voltage drop was registered at 0.25 r/m and 5.00 r/m, and the highest at 0 r/m and 10.00 r/m. For the remaining speed rotations, a clear differentiation could not be established. Even so, independent of pH variations at the cathode chamber, cathode rotation can lower voltage drop along the cathode side.

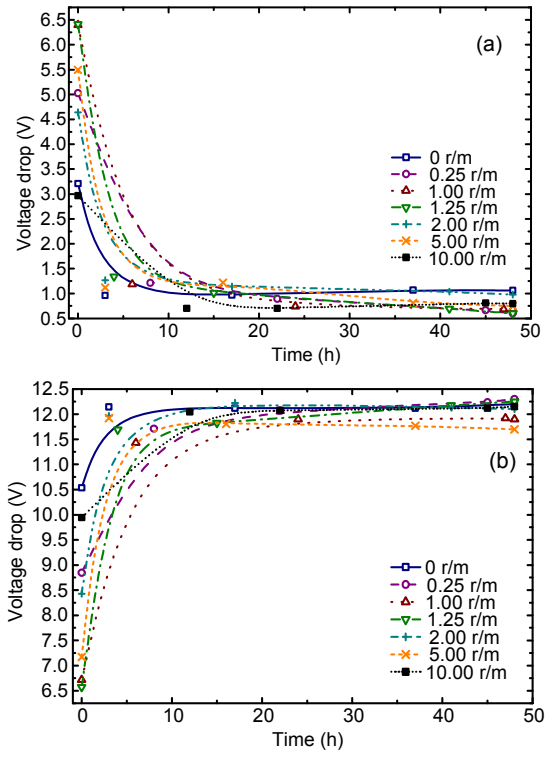

Fig. 9 Voltage drop vs. time along the cell on the anode side (a) and cathode side (b) at different cathode rotation speeds

Elevated voltage drop at the cathode side (Figs. 9a and 9b) implies low voltage across the anode side. As a consequence, the electric field was very weak on the anode side, which was reflected in low electromigration. Even when voltage drop values were very similar, there were low voltages at 0 r/m and 10.00 r/m. Higher voltage values were observed at 0.25 r/m and 1.00 r/m.

4.6 Future development and applications

The present work evaluated only one electrode configuration. Certainly, there are numerous other electrode configurations and speeds that could be useful for the migration of particles in porous media and need to be evaluated. Likewise, there might be other ways to alter the electric field orientation that would result in even higher performances than those presented in this study.

Since the path of a particle traveling through porous media is normally tortuous, the proposed technology could be applicable to electromigration of soluble, weakly dissociated or non-dissociated species driven by an electric field in any porous medium. In fact, it would be highly valuable to evaluate this new technology in soil chemistry, chromatography, ion exchange, electrophoresis, membrane technology, biotechnology and some other related fields. At present, we are dealing with the decontamination of soils.

Electrode rotation, as applied in this experiment, builds up a non-uniform electric field. An inhomogeneous electric field acts on both neutral and polarized particles. The investigation of the migration of polarizable species in inhomogeneous fields such as oils is also a potential field of application of this technology.

5 Conclusions

A constantly reoriented electric field can substantially increase cation electromigration in kaolin. The frequency at which the electric field is changed determines whether constant reorientation of the electric field is effective. For this experiment, the optimal reorientation in terms of cathode rotation speed was 1.25 r/m. When the rotation speed reached 10 r/m, metal migration was even lower than when the cathode was static (i.e., 0 r/m).

It appears that the constant reorientation of the electric field helps ions to find their way through connected pores in the pore matrix. In contrast, when the field has a single orientation, the probability of an ion making a net displacement towards either of the electrodes through an irregular network of pores, is substantially reduced.

Massive migration of ions brings about an increase in charge transport, which in turn causes more water splitting at the electrodes. This augmented transport of charge can be interpreted as a reduction in the electrical resistance of the porous matrix. Consequently, a stronger acid front develops, aiding the migration of cations towards the cathode.

References

Cox, C.D., Shoesmith, M.A., Gosh, M.M., 1996. Electrokinetic remediation of mercury-contaminated soils using iodine/iodide lixiviant. *Environmental Science & Technology*, **30**(6):1933-1938. [doi:10.1021/es950633r]

Eisenberg, M., Tobias, C.W., Wilke, C.R., 1954. Ionic mass transfer and concentration polarization at rotating electrodes. *Journal of the Electrochemical Society*, **101**(6): 306-320. [doi:10.1149/1.2781252]

Fabian, C., Ridd, M.J., Sheehan, M., 2006. Rotating cylinder electrode study of the effect of activated polyacrylamide on surface roughness of electrodeposited copper. *Hydrometallurgy*, **84**(3-4):256-263. [doi:10.1016/j.hydromet.2006.08.001]

Gabe, D.R., Wilcox, D.G., Gonzalez-Garcia, J., Walsh, F.C., 1998. The rotating cylinder electrode: its continued development and application. *Journal of Applied Electrochemistry*, **28**(8):759-780. [doi:10.1023/A:1003464415930]

Goering, R.V., 2010. Pulsed field gel electrophoresis: a review of application and interpretation in the molecular epidemiology of infectious disease. *Infection Genetics and Evolution*, **10**(7):866-875. [doi:10.1016/j.meegid.2010.07.023]

Humble, P.H., Harb, J.N., Tolley, H.D., Woolley, A.T., Farnsworth, P.B., Lee, M.L., 2007. Influence of transport properties in electric field gradient focusing. *Journal of Chromatography A*, **1160**(1-2):311-319. [doi:10.1016/j.chroma.2007.04.013]

Jacobs, R.A., Sengun, M.Z., Hicks, R.E., 1994. Model and experiments on soil remediation by electric fields. *Journal of Environ. Science and Health, Part A: Environmental Science and Engineering and Toxicology*, **29**(9): 1933-1955.

Lageman, R., Clarke, R.L., Pool, W., 2005. Electro-reclamation, a versatile soil remediation solution. *Engineering Geology*, **77**(3-4):191-201. [doi:10.1016/j.enggeo.2004.07.010]

Lemaire, T., Kaiser, J., Naili, S., Sansalone, V., 2010. Modeling of the transport in electrically charged porous media including ionic exchanges. *Mechanics Research Communications*, **37**(5):495-499. [doi:10.1016/j.mechrescom.2010.05.009]

Lorimer, J.P., Pollet, B., Phull, S.S., Mason, T.J., Walton, D.J., 1997. The effect upon limiting currents and potentials of coupling a rotating disc and cylindrical electrode with ultrasound. *Electrochimica Acta*, **43**(5-6):449-455. [doi:10.1016/S0013-4686(97)00126-6]

Moldrup, P., Olesen, T., Komatsu, T., Schjonning, P., Rolston, D.E., 2001. Tortuosity, diffusivity, and permeability in the soil liquid and gaseous phases. *Soil Science Society of America Journal*, **65**(3):613-623. [doi:10.2136/sssaj2001.653613x]

Nystroem, G.M., Ottosen, L.M., Villumsen, A., 2005. Electrodialytic removal of Cu, Zn, Pb and Cd from harbor sediment: influence of changing experimental conditions. *Environmental Science & Technology*, **39**(8):2906-2911. [doi:10.1021/es048930w]

Pamukcu, S., Weeks, A., Wittle, J.K., 2004. Enhanced reduction of Cr(VI) by direct electric current in a contaminated clay. *Environmental Science & Technology*, **38**(4): 1236-1241. [doi:10.1021/es034578v]

Perkin, F.M., 1906. A Simple Form of Rotating Electrode for Electrochemical Analysis. Faraday Society Conference, p.91-93. [doi:10.1039/tf9060200091]

Price, T.S., Judge, G.H., 1906. The electrolytic deposition of zinc, using rotating electrodes. *Transactions of the Faraday Society*, **2**:85-90. [doi:10.1039/tf9060200085]

Probstein, R.F., Hicks, R.E., 1993. Removal of contaminants from soils by electric fields. *Science*, **260**(5107):498-503. [doi:10.1126/science.260.5107.498]

Puig, P., Borrull, F., Calull, M., Aguilar, C., 2007. Recent advances in coupling solid-phase extraction and capillary electrophoresis (SPE-CE). *TrAC Trends in Analytical Chemistry*, **26**(7):664-678. [doi:10.1016/j.trac.2007.05.010]

Sadrzadeh, M., Razmi, A., Mohammadi, T., 2007. Separation of different ions from wastewater at various operation conditions using electrodialysis. *Separation and Purification Technology*, **54**(1):147-156. [doi:10.1016/j.seppur.2006.08.023]

Shen, L., Chen, Z., 2007. Critical review of the impact of tortuosity on diffusion. *Chemical Engineering Science*, **62**(14):3748-3755. [doi:10.1016/j.ces.2007.03.041]

Shen, Z., Chen, X., Jia, J., Qu, L., Wang, W., 2007. Comparison of electrokinetic soil remediation methods using one fixed anode and approaching anodes. *Environmental Pollution*, **150**(2):193-199. [doi:10.1016/j.envpol.2007.02.004]

Sinnott, R.K., 1983. Chemical Engineering, 3rd Edition, Chemical Engineering Design. Butterworth-Heinemann, Germany.

Tsang, Y.W., 1984. The effect of tortuosity on fluid flow through a single fracture. *Water Resources Research*, **20**(9):1209-1215. [doi:10.1029/WR020i009p01209]

US EPA (US Environmental Protection Agency), 1986. Test

Methods for Evaluating Solid Waste, 3rd Edition, Vol. 1A, Laboratory Manual, Physical/Chemical Methods, SW-846. Office of Solid Waste and Emergency Response, Washington DC.

Virkutyte, J., Sillanpaa, M., 2007. The hindering effect of experimental strategies on advancement of alkaline front and electroosmotic flow during electrokinetic lake sediment treatment. *Journal of Hazardous Materials*, **143**(3): 673-681. [doi:10.1016/j.jhazmat.2007.01.014]

Wang, J.Y., Huang, X.J., Kao, J., Stabnikova, O., 2007. Simultaneous removal of organic contaminants and heavy metals from kaolin using upward electrokinetic soil remediation process. *Journal of Hazardous Materials*, **144**(1-2):292-299. [doi:10.1016/j.jhazmat.2006.10.026]

Wilson, I.R., 2004. Kaolin and halloysite deposits of China. *Clay Minerals*, **39**(1):1-15. [doi:10.1180/0009855439 10116]

Yeung, A.T., Hsu, C.N., Menon, R.M., 2011. Electrokinetic extraction of lead from kaolinites: I numerical modeling. *The Environmentalist*, **31**(1):33-38. [doi:10.1007/s10669-010-9298-1]

Yuan, C., Weng, C.H., 2006. Electrokinetic enhancement removal of heavy metals from industrial wastewater sludge. *Chemosphere*, **65**(1):88-96. [doi:10.1016/j. chemosphere.2006.02.050]